

Article

Biomagnetic monitoring of the spatial distribution of atmospheric particulate matter in an industrialized city in Japan: Case study at Muroran

Kazuo Kawasaki^{1,*}, Nagisa Sawada²¹ Faculty of Sustainable Design, University of Toyama, Toyama 930-8555, Japan² Graduate School of Science and Engineering, University of Toyama, Toyama 930-8555, Japan* **Corresponding author:** Kazuo Kawasaki, kawasaki@sus.u-toyama.ac.jp

CITATION

Kawasaki K, Sawada N. Biomagnetic monitoring of the spatial distribution of atmospheric particulate matter in an industrialized city in Japan: Case study at Muroran. *Pollution Study*. 2024; 5(2): 2931.
<https://doi.org/10.54517/ps.v5i2.2931>

ARTICLE INFO

Received: 5 September 2024

Accepted: 16 October 2024

Available online: 25 November 2024

COPYRIGHT



Copyright © 2024 by author(s).

Pollution Study is published by Asia Pacific Academy of Science Pte. Ltd.

This work is licensed under the Creative Commons Attribution (CC BY) license.

<https://creativecommons.org/licenses/by/4.0/>

Abstract: Japan has 111 active volcanoes, supplying a great amount of magnetically-enhanced fly ashes. Such fly ashes likely mask anthropogenic magnetic signals; therefore, only a few magnetic biomonitoring studies have been reported in active volcanic regions, including Japan. The environmental magnetic results are reported for the materials deposited on Sasa Kurilensis, also known as dwarf bamboo, in the vicinity of the industrialized Muroran city center in Japan. The dust on the ten leaves at 105 sites was wiped off with a commercial wipe sheet, and their rock magnetic properties were analyzed. Room- and low-temperature magnetic analyses indicate that the major magnetic mineral in the dust is partially oxidized magnetite, ranging from single to pseudo single domain size, and the magnetic mineralogy on the leaves' surface remains consistent throughout the study area. Much higher saturation isothermal remanent magnetization intensities are observed in the city's eastern parts. The dominant wind directions in Muroran city are northwest, indicating that the steel companies in the city center are the major source of the fine-grained magnetic minerals on the dwarf bamboo leaves. These results indicate that using the leaves of dwarf bamboo for magnetic biomonitoring can be a non-destructive and rapid method to study the spatial distribution of atmospheric particulate matter from local industrial activities, even in active volcanic areas.

Keywords: environmental magnetism; oxidized magnetite; active volcanic region; steel manufacture; dwarf bamboo

1. Introduction

Airborne magnetic minerals are generated by various industrial processes; thereby, the magnetic properties of these minerals, including magnetic mineralogy, quantity, and grain size, can serve as pivotal indicators of industrial contaminants [1]. Environmental magnetic monitoring techniques have emerged as non-destructive, expeditious, and cost-effective measures for evaluating different types of anthropogenic pollution [for a review and references within [2]. Early environmental magnetic studies on pollution focused on the spatial distribution of anthropogenic magnetic minerals and heavy metal concentrations such as lead and zinc, showing that magnetic properties can be used as a proxy for heavy metal concentrations [3,4]. Könczöl et al. [5] reported that exposure of human alveolar epithelial-like type-II cells to very fine magnetite that can be found in airborne particulate matter enhanced reactive oxygen species production. Further, the concentrations of ultrafine magnetite in the brain tissues are higher in either the Alzheimer's disease brain [6] or brain tumor tissues [7]. Although ferritin is the primary intracellular iron storage protein [8], Maher et al. [9] found that anthropogenic fine magnetite can enter directly into the human brain via the olfactory nerve. Externally sourced fine magnetic minerals could pose a

hazard to human health. Biomagnetic magnetic monitoring methods, including tree leaves, tree bark, and moss, have been shown to be effective and reliable in monitoring fine magnetic particles worldwide. Fabian et al. [10] reported the magnetic properties of terrestrial moss samples (*Hylocomium splendens*) in Oslo, Norway, and found urban dust enhancement in urban areas. Castañeda-Miranda et al. [11] reported successful biomagnetic monitoring results in seasons with no or low rainfall using leaves of *Ficus benjamina* in Querétaro, Mexico. Based on detailed rock magnetic experiments and dendrochronology, Zhang et al. [12] found that there was a positive correlation between saturation isothermal remanent magnetization (SIRM) values of *Salix matsudana* tree ring cores and the annual iron production of the smelting factory in Xinglong County, China. However, few studies have reported environmental magnetic monitoring in Japan and all of them are carried out along the road to estimate roadside pollution by passing vehicles [13–15]. Therefore, it is important to test if biomagnetic monitoring methods can be used to determine the local spatial distribution of fine magnetite in Japan. The small number of studies is due to the significant amount of magnetically-enhanced fly ashes from volcanoes and the dense population causing high magnetic noise levels. Kawasaki et al. [14] reported that biomagnetic techniques could be practical tools to monitor pollution associated with vehicle traffic, even in Japan, and the *Sasa Kurilensis*, or dwarf bamboo, can effectively collect roadside dust. This study aims to a) test if the biomagnetic method using *Sasa Kurilensis* is adequate to determine urban air pollution even in active volcanic regions and b) determine the spatial distribution of air pollution around the industrialized city center of Muroran, Japan.

2. Materials and methods

2.1. Study area

Muroran, a heavy industrial city in Japan, is located in southwestern Hokkaido, Japan, and the city's total area is 80.65 km². Muroran has developed mainly with the steel industry but also shipbuilding, coal forwarding, and oil refining. This city is known as “the city of steel” in Japan. Two major steel companies, equipping coke-oven plant and blast furnace, are located in the central part of the city (**Figure 1**). Muroran city was constructed with broad streets to create a greenbelt for the air defense system and fire prevention installations as well as for citizens' health and recreation [16].

The geology in the study area was mainly formed by Quaternary sediments, a Neogene-Tertiary Muroran formation, and Washibetsu Dake andesite [17]. The Shiomi Park and Chiribetsu Park are located on Quaternary sediments consisting of soil, clay, silt, sand, and peat. The Sokuryozan and Cape Chikyu are located on the Neogene-Tertiary Muroran formation, which consists of pyroclastic rocks, including andesitic and liparitic tuffaceous agglomerate. The Washibetsu Dake is a Middle Pleistocene andesitic composite volcano.

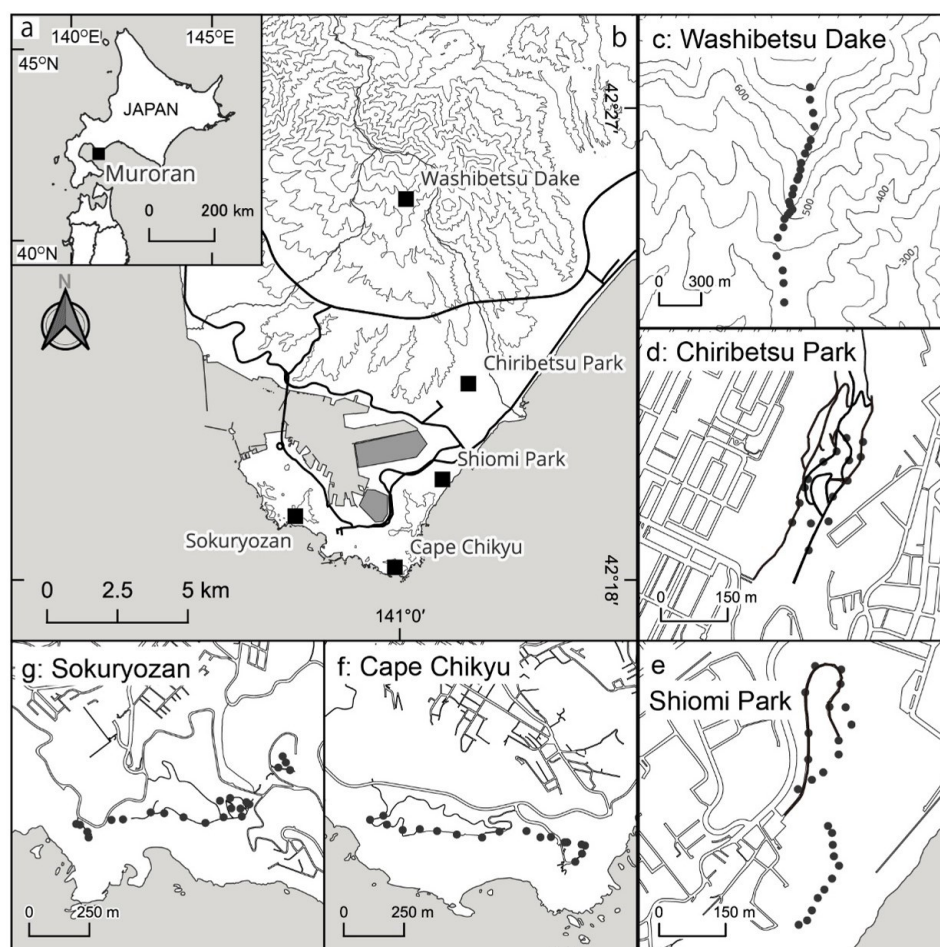


Figure 1. (a) A broad map showing the study area; (b) a regional map showing five natural parks. Dark grey hatches show major steel industries; (c) Washibetsu Lake site with sampling locations; (d) Chiribetsu Park site with sampling locations; (e) Shiomis Park site with sampling locations; (f) Cape Chikyu site with sampling locations; (g) Sokuryozan site with sampling locations.

The thick lines in (b) are major roads. The thin lines in (b) and (c) are contour lines. The black line in (d) to (g) is pathways where cars are not allowed. The solid circles in (c) to (g) are sampling sites.

Kakimoto et al. [18] reported the concentration ratio of dinitropyrenes (DNPs) to 1-nitropyrene (1-NP) for Muroan city. They implied that the air of Muroan was relatively polluted with polycyclic aromatic hydrocarbons (PAHs) that were emitted from both diesel exhaust and exhaust from the steel and coke manufacturing plants. Recently, Hayakawa et al. [19] measured total suspended particulates collected for two weeks in Muroan and found that the atmospheric PAHs concentration was higher when the wind blew from the coke-oven plant. In addition, they mentioned that the observed 1-NP values were close to those observed in particulates from coal combustion systems rather than automobiles.

2.2. Sampling

Two different sampling methods were used to collect materials deposited on the leaves of *Sasa Kurilensis*. The first method involved wiping the materials off with a sheet of commercial ethanol wipe paper measuring 19.4 mm in width and 13.2 mm in

height for conventional environmental magnetic analysis. The leaves of the dwarf bamboo, which have an oval shape with a major axis of approximately 17 cm and a minor axis of approximately 5 cm at a height of around 1 m from the ground level, were selected for the study. Leaves not covered by another leaf are selected within a radius of about 3 m. All sites except five sites near the parking area at Cape Chikyu are located near the pathways where cars are not allowed at each park. Ten of these leaves were wiped off with a single wipe sheet, resulting in each sheet sample containing the combined dust from the set of leaves mentioned above. One hundred-five specimens were collected from five local nature parks: Chiribetsu Park, Shiomi Park, Cape Chikyu, Sokuryozan, and Washibetsu Dake, all surrounding the city center of Muroran (**Figure 1**), resulting in 105 specimens in total. The second method used a silica wool dampened with ethanol for low-temperature experiments. Similarly, another ten leaves were wiped off with this silica wool at selected sites. Note that the “dirty” wipe sheet was placed directly into a 7 cm³ non-magnetic plastic cube for room-temperature rock magnetic measurements, and the silica wool was placed into a plastic bag with a zipper. All magnetic measurements were conducted in the rock magnetic laboratories at the University of Toyama.

2.3. Room-temperature experiments

The relative amounts of magnetic minerals, mineralogy, and grain size were determined using stepwise isothermal remanent magnetization (IRM) acquisition analysis, followed by stepwise alternating field (AF) demagnetization. All samples underwent pulsed magnetization in 11 direct current (DC) field steps up to 1200 mT using a Magnetic Measurements PM9 pulse magnetizer, followed by AF demagnetization in 9 steps up to 70 mT. The study defines remanence saturation intensity (J_{sat}) as 90% of the maximum intensity at 1200 mT. Remanent magnetizations of the specimens were measured using a 2G Enterprises 750 SQUID magnetometer equipped with an in-line alternating field demagnetizer.

2.4. Low-temperature experiments

Magnetic mineralogy in silica wool samples was determined by low-temperature analysis using a Quantum Design magnetic property measurement system (MPMS) XL. Two samples, after drying at room temperature, at each nature park were magnetized in a 1500 mT DC field at 5 K and monitored during zero-field heating to 300 K at every 5 K.

2.5. Microscopic characteristics

Scanning electron microscope (SEM) analyses were carried out on 2–4 samples from each nature park to identify the magnetic materials in the dust collected from “dirty” wiper sheets. A neodymium magnet was used to extract the magnetic materials. The quick evaporation of ethanol from the wiper paper enabled the smooth release of materials. The SEM observations were conducted using a Hitachi Miniscope TM3030.

3. Results

3.1. Room-temperature experiments

The rapid acquisition of IRM to saturation by 200 mT but not at 100 mT is observed for all specimens (**Figure 2a**). The remanent intensity decreases by approximately 80% when the AF field is 30–40 mT and about 90% at around 70 mT (**Figure 2b**), indicating that major magnetic minerals are low-coercivity minerals. Although the AF curves differed by up to 10%–15%, this was not likely due to differences in magnetic minerals but rather to differences in the mixing ratio of different domain sizes. Overall, these characteristics are typical of pseudosingle-domain (PSD) magnetite [20]. Based on hysteresis measurements, Jordanova et al. [21] reported that the anthropogenic magnetite collected in Burga, Republic of Bulgaria, is likely delivered from industrial combustion and exhaust emissions and is in a PSD state. There are no discernible differences in the magnetic behaviors observed by IRM acquisition and AF demagnetization among the five natural parks.

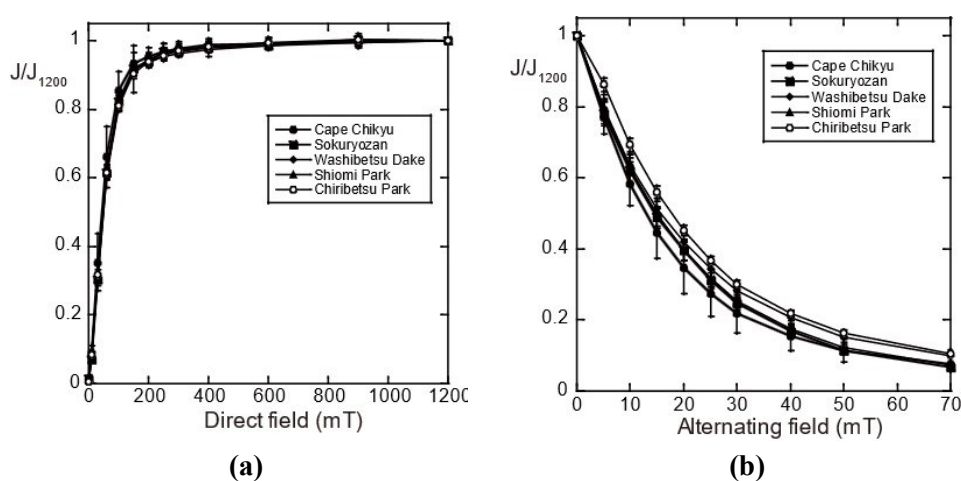


Figure 2. Room-temperature magnetic measurements for specimens at each native park. **(a)** Averaged isothermal remanent magnetization (IRM) acquisition curves with their standard deviation; **(b)** averaged alternating field demagnetization curves with their standard deviation. J_{1200} is the remanent intensity (J) value at 1200 mT.

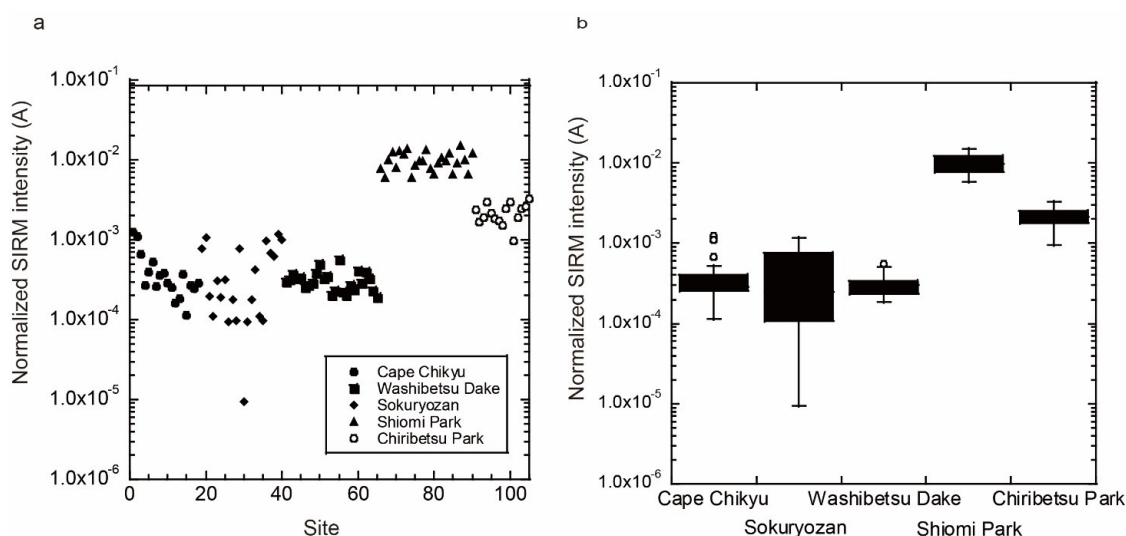


Figure 3. **(a)** Saturation IRM (SIRM) intensities for all specimens; **(b)** whisker plot for each park. SIRM intensities are normalized by the surface area of leaves.

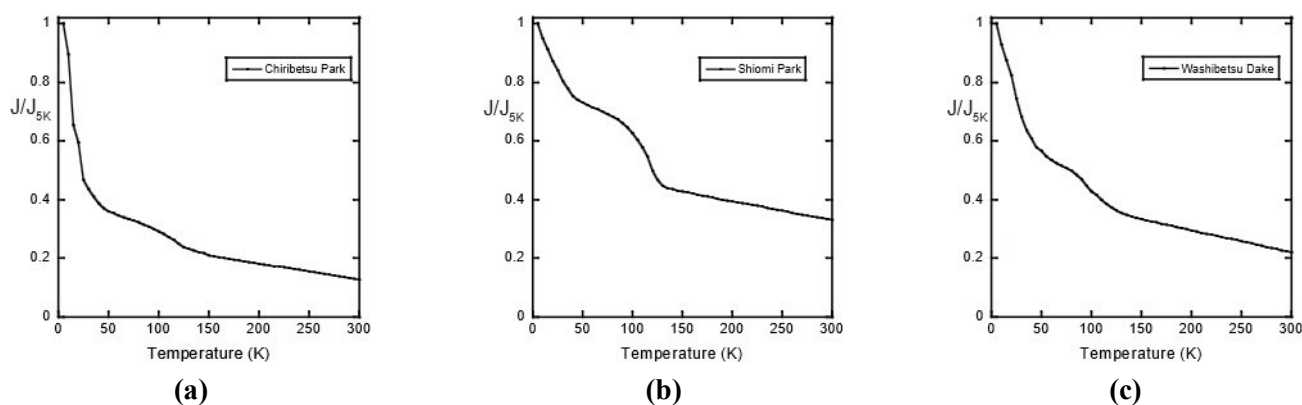
The median SIRM intensities normalized by leaf area for Chiribetsu Park, Shiomi Park, Cape Chikyu, Sokuryozan, and Washibetsu Dake are in **Table 1**. The median SIRM intensity for Cape Chikyu, Sokuryozan, and Washibetsu Dake are the same in order of magnitude. Chiribetsu Park shows an order of magnitude higher SIRM intensity than these three parks, and Shiomi Park shows two orders of magnitude higher SIRM intensity than those three parks (**Figure 3a,b**).

Table 1. The median saturation isothermal remanent magnetization (SIRM) intensity for the studied nature park. SIRM intensities are normalized by the surface area of leaves.

Nature Park	Number of sites	Median SIRM intensity (A)	Quartiles	
			Q_1	Q_3
Chiribetsu Park	15	9.50×10^{-6}	7.91×10^{-5}	1.11×10^{-5}
Shiomi Park	25	4.27×10^{-5}	3.42×10^{-5}	5.41×10^{-5}
Cape Chikyu	18	1.28×10^{-6}	1.13×10^{-6}	1.75×10^{-6}
Sokuryozan	22	1.10×10^{-6}	4.85×10^{-7}	3.31×10^{-6}
Washibetsu Dake	25	1.33×10^{-6}	1.03×10^{-6}	1.52×10^{-6}

3.2. Low-temperature experiments

Overall, the IRM of all ten samples decreases rapidly from 5 K to around 40 K, then decreases more slowly between approximately 40 K and 110 K, and decreases rapidly again from around 110 K to 120 K (**Figure 4a–e**). This pattern of decay indicates that the magnetic minerals in the sample are oxidized magnetite or maghemite, with some magnetite present [22,23]. The IRM curve of the sample from Chiribetsu Park shows a steeper intensity drop after 5 K than the samples from other parks. The sharp intensity drop indicates the presence of superparamagnetic (SP) minerals [24], and therefore, the dust at Chiribetsu Park likely contains ultrafine magnetic minerals. The clear IRM decreases around 120 K, which is likely a Verwey transition [25], indicating the presence of magnetite. The results show that the predominant magnetic minerals of dust on leaves' surface are partially oxidized magnetite with some magnetite and ultrafine magnetic minerals.



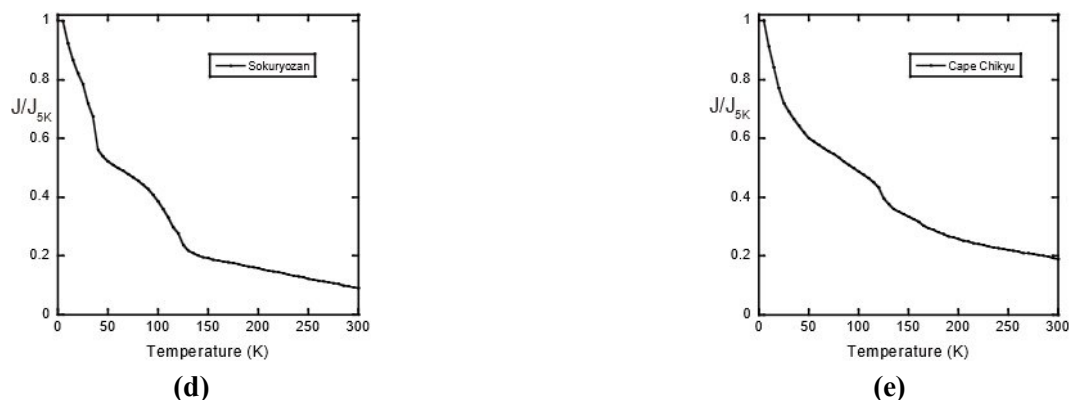


Figure 4. Low-temperature curves for selected samples from: **(a)** Chiribetsu Park; **(b)** Shiomi Park; **(c)** Washibetsu Dake; **(d)** Sokuryozan; **(e)** Cape Chikyū. J_{5K} is the remanent magnetization intensity (J) at 5K.

3.3. Microscopic characteristics

The SEM analyses of 26 samples determine two morphologies of grains: angular/aggregate particles (**Figure 5a,c**) and spherical particles (**Figure 5a,b,d**). Some aggregate particles contain smaller angular and/or spherical particles (**Figure 5a,d**). Both morphologies are found at all five nature parks although spherical particles were found more in Chiribetsu Park and Shiomi Park than other three parks.

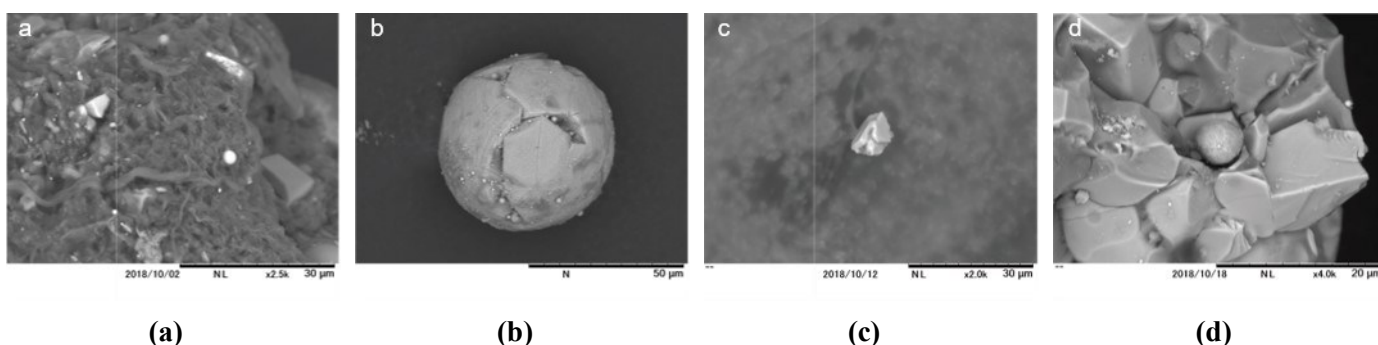
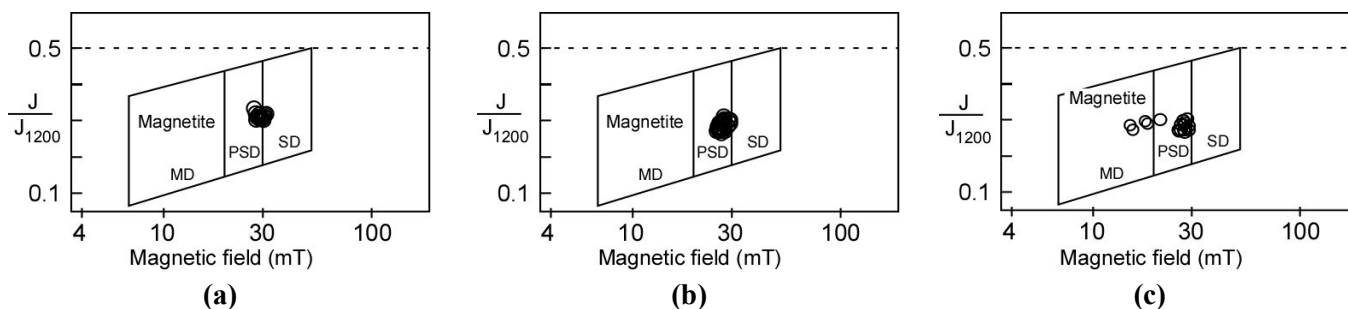


Figure 5. Representative results of SEM photographs of magnetic particles separated from selected dust samples **(a)** from Cape Chikyū; **(b)** from Chiribetsu Park; **(c)** from Shiomi Park; **(d)** from Shiomi Park.

4. Discussion



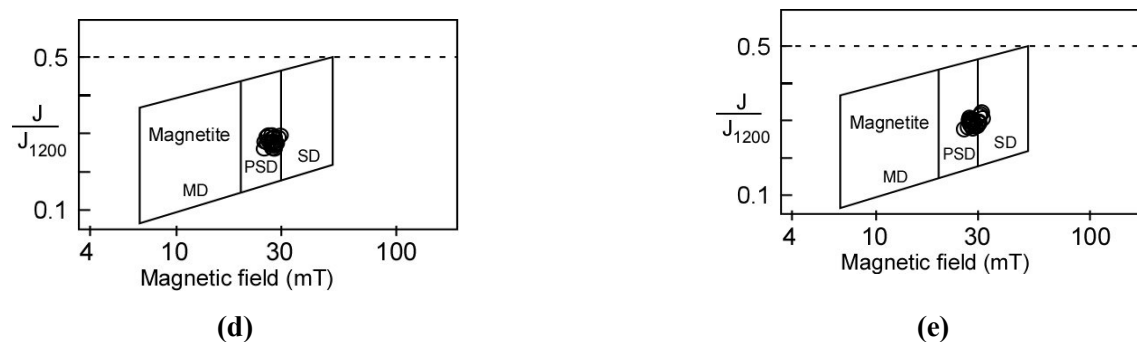


Figure 6. Crossover plot for all samples at each native park. **(a)** Chiribetsu Park; **(b)** Shiomi Park; **(c)** Cape Chikyu; **(d)** Sokuryozan; **(e)** Washibetsu Dake. The magnetite-type plot of Symons and Cioppa [20] is used.

In the study area, the main magnetic minerals in the dust particles deposited on plant leaves are surface-oxidized magnetite and/or maghemite based on the acquisition curves of IRM, decay curves of AF demagnetization, and low-temperature measurements. The consistent characteristics of the magnetic minerals on leaves throughout the study area indicate that the crossover plot analysis [20] can be used to estimate the magnetic domain or grain size using the crossover points of the IRM acquisition and subsequent AF demagnetization curves. The magnetite-type plot is selected due to the close coercivity between magnetite and maghemite or slightly oxidized magnetite [26]. All observed crossover points except five sites from Cape Chikyu fall in a similar region of the PSD-SD magnetite area (**Figure 6**), indicating that magnetic grain size is consistent throughout the study area. Note that crossover points of five exceptional sites from Cape Chikyu fall in the region of the MD magnetite area. Kawasaki et al. [15] reported that the coarser particles are found closer to the roadside in areas where cars are the primary source of pollution, and these five sites are located near the parking area. The results indicate that dust on leaves at these five sites likely contains iron particles directly derived from local vehicles, and therefore, these sites are excluded for further discussion.

The dust on the leaves' surface likely has similar magnetic mineralogy and grain sizes across locations, suggesting that the observed SIRM intensity can proxy for the relative amounts of magnetic minerals. Sasa Kurilensis is an evergreen tree, and each leaf's exposure time cannot be determined. However, Sasa Kurilensis is a highly clonal, monocarpic plant that dies off after gregarious flowering [27]. No mosaic patterned in unflowered bamboo and die-off bamboo patches is reported in Muroran, indicating that the studied Sasa Kurilensis are similar in age. Dust on the ten leaves is collected at each site, and the observed specimen's SIRM intensity is not significantly different within the same natural park. The exact age of each Sasa Kurilensis is unknown; however, the observed SIRM intensities have been well averaged out, and we deem them representative values for each site. The median SIRM intensities of the Cape Chikyu, Sokuryozan, and Washibetsu Dake are similar in values. Conversely, the median SIRM intensities of Chiribetsu Park and Shiomi Park show about an order or two orders of magnitude higher than the median SIRM intensities of these three sites, respectively. The Chiribetsu Park is about 2.5 km northeast of the central part of the city, where two major steel companies are located, and the Shiomi Park is about 2 km southeast of the city center.

The SEM observations show that the particles contain both angular/aggregate and rounded/spherical grains (**Figure 5**). Spherical-shaped magnetic particles are typical of the particles formed by solid fuel combustion and, thereby, of anthropogenic origin [28]. Machemer [29] reported that iron particles formed by blast furnace processes at iron and steel manufacturing facilities consist of hematite, magnetite, and maghemite. These iron particles are predominantly spheres of iron that have diameters from submicrometers to tens of micrometers. Conversely, angular/aggregate particles are more likely to be emitted from vehicle emissions [30]. Furthermore, non-spherical particles can originate from sources such as exhaust emissions, braking systems, and the frictional wear or corrosion of body and engine materials [31,32].

Japan has 111 active volcanoes, and eight active volcanoes exist within a 100 km radius of Muroran. Three of them had erupted with volcanic ash in the last 50 years, i.e., a) Hokkaido Komagatake in 2000, about 45 km southwest of Muroran; b) Usu Zan in 2000, about 25 km northwest of Muroran; and c) Tarumae San in 1981, about 55 km northeast of Muroran [33]. However, Shiomi Park, where the highest SIRM intensity was observed, is not close to any of the three volcanoes. In addition, Kawasaki et al. [13] reported that topsoils in the volcanic area contain titanomagnetite even near the roadside. No IRM drops around 50–80 K, where titanomagnetite shows intensity decreases [34], are observed for all specimens in low-temperature experiments, indicating that negligible titanomagnetites are in the dust on the leaves in the Muroran area. Hence, the impact of volcanic ash is minimal, and the studied area is more likely to have been affected by local factors, such as geology and human activities. Shiomi Park and Chiribetsu Park, where higher SIRM intensities were observed, have geological backgrounds different from those of the other sites. These two parks are mainly Quaternary sediments, while the other three parks are either andesitic pyroclastic rocks or andesite. Conversely, there is no significant difference in the magnetic minerals found in the five nature parks. In particular, titanomagnetite, commonly found in volcanic rocks, was not found at these parks. Therefore, the studied area is more likely to have been affected by local human activities.

The Japan Meteorological Agency (JMA) reported the observed days of Asian dust between 1967 and 2024 based on the visibility measurement [35], and a relatively small number of such days are reported for the Hokkaido area. The number of Asian dust days in 2017 in Muroran is two, on the 7th and 8th of May. The Hybrid Single-Particle Lagrangian Integrated Trajectory (HYSPPLIT) model [36,37] is used to estimate the potential transport pathways of the observed Asian dust in Muroran. The result shows that the air parcels originated from western Mongolia (**Figure 7**). Therefore, the observed magnetic minerals could originate from Asian dust carried by the westerly jet stream and winter monsoons from arid regions in China and Mongolia [38]. Tsuchiya et al. [39] reported that the Asian dust inflow is characterized by a high partially oxidized SD-PSD magnetite concentration. The main magnetic minerals characterized in this study area are surface-oxidized magnetite and/or maghemite and show good agreement with the magnetic minerals in the Asian dust. However, the SIRM intensities are higher on the eastern side of the city center, and such distributions are highly unlikely to be caused by atmospheric acidic pollutants transported from the Asian continent over long distances. Hence, we conclude that the magnetic minerals in the dust on plant leaves originated from local activities rather than Asian dust.

Li et al. [40] reported that iron and steel production is a major source of atmospheric magnetic particle emissions. They also noted that fuel combustion only comprises less than 13% of the overall atmospheric magnetic particle emissions. In this study, Chiribetsu Park and Shiomi Park samples show much higher SIRM intensities than the other three sites. The dominant wind direction in Muroran between 1991 and 2020 is northwest (**Table 2**), and no rainfall event (≤ 0.0 mm/hour) was observed during the seven days before sampling. These two parks are on the downwind side of the city center, where the two steel companies are located, indicating that these steel companies are the main source of dust on the dwarf bamboo leaves. Furthermore, the observed higher SIRM intensities on the downwind of the city center agree with the previously reported atmospheric PAHs concentration and 1-Np values [16].

Table 2. Mean wind speed and most frequent wind direction in Muroran city between 1991 and 2020 [41].

Month	Mean wind speed (m/s)	Most frequent wind direction
January	5.7	NW
February	5.2	NW
March	4.9	NW
April	4.4	NW
May	4.1	ENE
June	3.7	ENE
July	3.6	ENE
August	3.5	ENE
September	3.9	NW
October	4.7	NW
November	5.6	NW
December	6.1	NW

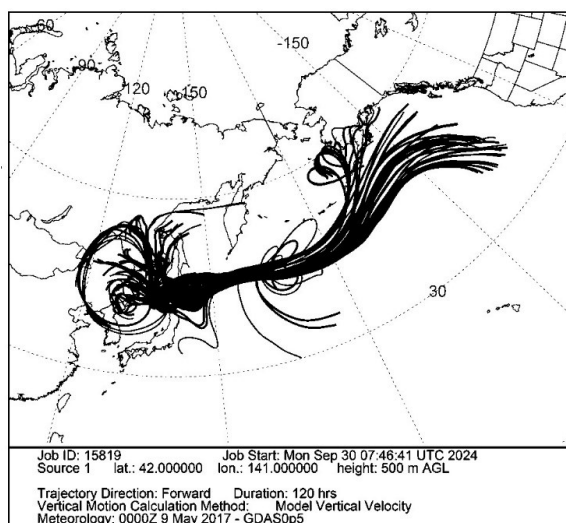


Figure 7. The hybrid single-particle lagrangian integrated trajectory model for the study area.

5. Conclusion

The main magnetic minerals found in the dust on leaves throughout Muroran city are fine-grained partially oxidized magnetite, based on IRM acquisition tests, AF demagnetization behaviors, low-temperature curves, and crossover plot analyses. The observed SIRM distributions show higher intensities in the city's eastern parts. The dominant northwest wind directions in Muroran city indicate that the two steel companies in the city center are the main source of the fine-grained magnetic minerals on the dwarf bamboo leaves rather than Asian dust or geological background. The results show the potential of *Sasa Kurilensis*, which is widespread across East Asia, as a subject for investigating the detailed spatial distribution of urban air pollution.

Author contributions: Conceptualization, KK and NS; methodology, KK; validation, KK; formal analysis, KK and NS; investigation, KK; resources, KK; data curation, KK; writing—original draft preparation, KK; writing—review and editing, KK and NS; visualization, KK and NS; project administration, KK; funding acquisition, KK. All authors have read and agreed to the published version of the manuscript.

Funding: This research was partially funded by JSPS KAKENHI, grant number JP 23K03545.

Acknowledgments: The authors gratefully thank: Hiroki Shibata for his help with magnetic measurements, two reviewers for very helpful comments that have greatly improved this paper, and the NOAA Air Resources Laboratory (ARL) for the provision of the HYSPLIT transport and dispersion model and/or READY website (<https://www.ready.noaa.gov>) used in this publication.

Conflict of interest: The authors declare no conflict of interest.

References

1. Evans M, Heller F. Environmental magnetism: principles and applications of enviromagnetics. Academic press; 2003
2. Hofman J, Maher BA, Muxworthy AR, et al. Biomagnetic monitoring of atmospheric pollution: a review of magnetic signatures from biological sensors. *Environmental Science & Technology*. 2017, 51(12): 6648-6664.
3. Heller F, Strzyszczyk Z, Magiera T. Magnetic record of industrial pollution in forest soils of Upper Silesia, Poland. *Journal of Geophysical Research: Solid Earth*. 1998, 103: 17767-17774.
4. Hoffmann V, Knab M, Appel E. Magnetic susceptibility mapping of roadside pollution. *Journal of Geochemical Exploration*. 1999, 66: 313-326.
5. Könczöl M, Weiss A, Stangenberg E, et al. Cell-cycle changes and oxidative stress response to magnetite in A549 human lung cells. *Chemical research in toxicology*. 2013, 26: 693-702.
6. Pankhurst Q, Hautot D, Khan N, et al. Increased levels of magnetic iron compounds in Alzheimer's disease. *Journal of Alzheimer's disease*. 2008, 13: 49-52.
7. Brem F, Hirt AM, Winklhofer M, et al. Magnetic iron compounds in the human brain: a comparison of tumour and hippocampal tissue. *Journal of The Royal Society Interface*. 2006, 3: 833-841.
8. Arosio P, Levi S. Ferritin, iron homeostasis, and oxidative damage. *Free Radical Biology and Medicine*. 2002, 33: 457-463.
9. Maher BA, Ahmed IA, Karloukovski V, et al. Magnetite pollution nanoparticles in the human brain. *Proceedings of the National Academy of Sciences*. 2016, 113: 10797-10801.
10. Fabian K, Reimann C, McEnroe SA, et al. Magnetic properties of terrestrial moss (*Hylocomium splendens*) along a north-south profile crossing the city of Oslo, Norway. *Science of the Total Environment*. 2011, 409: 2252-2260.

11. Castañeda-Miranda AG, Chaparro MA, Pacheco-Castro A, et al. Magnetic biomonitoring of atmospheric dust using tree leaves of *Ficus benjamina* in Querétaro (México). *Environmental Monitoring and Assessment*. 2020, 192: 382.
12. Zhang C, Huang B, Piper JD, et al. Biomonitoring of atmospheric particulate matter using magnetic properties of *Salix matsudana* tree ring cores. *Science of the Total Environment*. 2008, 393: 177-190.
13. Kawasaki K, Horikawa K, Sakai H. Environmental Magnetism of Roadside Soil Contamination in the Restricted Bijyodaira Area of Mt. Tateyama, Toyama, Japan. *Asian Journal of Water, Environment and Pollution*. 2015, 12: 1-11.
14. Kawasaki K, Horikawa K, Sakai H. Magnetic biomonitoring of roadside pollution in the restricted Midagahara area of Mt. Tateyama, Toyama, Japan. *Environmental Science and Pollution Research*. 2017, 24(11): 10313-10325.
15. Kawasaki K, Fukushi K, Sakai H. Magnetic measurements of roadside topsoil pollution in an active volcanic region: Mt. Hakusan, Japan. *Water and Environment Journal*. 2018, 32(4): 556-565.
16. Nakano S, Kaku S, Nakae K, et al. Relationship Between Industrial Development and City Planning in Company Towns of the Japanese Steel Industry During World War II A case study of Muroran, Kamaishi, Hirohata and Yahata. *Urban and Regional Planning Review*. 2016, 3: 163-186.
17. Sawada Y. The Subsurface Geological Structure of the Alluvial Plain of Muroran, Hokkaido. *Science reports of the Tohoku University*. 2nd series, Geology. 1973. 6: 477-488
18. Kakimoto H, Kitamura M, Matsumoto Y, et al. Comparison of atmospheric polycyclic aromatic hydrocarbons and nitropolycyclic aromatic hydrocarbons in Kanazawa, Sapporo and Tokyo. *Journal of Health Science*. 2000, 46(1): 5-15.
19. Hayakawa K, Tang N, Morisaki H, et al. Atmospheric polycyclic and nitropolycyclic aromatic hydrocarbons in an iron-manufacturing city. *Asian Journal of Atmospheric Environment*. 2016, 10(2): 90-98.
20. Symons DTA, Cioppa MT. Crossover plots: a useful method for plotting SIRM data in paleomagnetism. *Geophysical Research Letters*. 2000, 27: 1779-1782.
21. Jordanova D, Jordanova N, Lanos P, et al. Magnetism of outdoor and indoor settled dust and its utilization as a tool for revealing the effect of elevated particulate air pollution on cardiovascular mortality. *Geochemistry, Geophysics, Geosystems*, 2012. 13: Q08Z49.
22. Özdemir Ö, Dunlop DJ, Moskowitz BM. The effect of oxidation on the Verwey transition in magnetite. *Geophysical Research Letters*. 1993, 20: 1671-1674.
23. Kosterov A. Low-temperature magnetization and AC susceptibility of magnetite: effect of thermomagnetic history. *Geophysical Journal International*. 2003, 154(1): 58-71.
24. Moskowitz BM, Bazylinski DA, Egli R, et al. Magnetic properties of marine magnetotactic bacteria in a seasonally stratified coastal pond (Salt Pond, MA, USA). *Geophysical Journal International*. 2008, 174: 75-92.
25. Verwey E, Haayman P. Electronic conductivity and transition point of magnetite (Fe_3O_4). *Physica*. 1941, 8: 979-987.
26. Peters C, Dekkers M. Selected room temperature magnetic parameters as a function of mineralogy, concentration and grain size. *Physics and Chemistry of the Earth, Parts A/B/C*. 2003, 28(16): 659-667.
27. Matsuo A, Tomimatsu H, Sangetsu Y, et al. Genet dynamics of a regenerating dwarf bamboo population across heterogeneous light environments in a temperate forest understorey. *Ecology and Evolution*. 2018, 8: 1746-1757.
28. Petrovský E, Kapička A, Jordanova N, et al. Low-field magnetic susceptibility: a proxy method of estimating increased pollution of different environmental systems. *Environmental Geology*. 2000, 39(3): 312-318.
29. Machermer SD. Characterization of airborne and bulk particulate from iron and steel manufacturing facilities. *Environmental Science & Technology*. 2004, 38(2): 381-389.
30. Bučko MS, Mattila OP, Chrobak A, et al. Distribution of magnetic particulates in a roadside snowpack based on magnetic, microstructural and mineralogical analyses. *Geophysical Journal International*. 2013, 195(1): 159-175.
31. Matzka J, Maher BA. Magnetic biomonitoring of roadside tree leaves: identification of spatial and temporal variations in vehicle-derived particulates. *Atmospheric Environment*. 1999, 33(28): 4565-4569.
32. Lu S, Wang H, Guo J. Magnetic enhancement of urban roadside soils as a proxy of degree of pollution by traffic-related activities. *Environmental Earth Sciences*. 2011, 64(2): 359-371.
33. Geological Survey of Japan, AIST (Ed.). *Catalog of Eruptive Events during the Last 10,000 Years in Japan, Version 2.3*. Geological Survey Japan, AIST. 2017.
34. Moskowitz BM, Jackson M, Kissel C. Low-temperature magnetic behavior of titanomagnetites. *Earth and Planetary Science Letters*. 1998, 157: 141-149.

35. Data collection of Asian Dust by Japan Meteorological Agency (in Japanese). Available online: https://www.data.jma.go.jp/gmd/env/kosahp/kosa_data_index.html (accessed on 2 October 2024).
36. Stein AF, Draxler RR, Rolph GD, et al. NOAA's HYSPLIT atmospheric transport and dispersion modeling system. *Bulletin of the American Meteorological Society*. 2015. 96: 2059-2077.
37. Rolph G, Stein A, Stunder B. Real-time environmental applications and display system: READY. *Environmental Modelling & Software*. 2017, 95: 210-228.
38. Kim W, Doh SJ, Yu Y. Asian dust storm as conveyance media of anthropogenic pollutants. *Atmospheric Environment*. 2012, 49: 41-50.
39. Tsuchiya N, Kato S, Kawasaki K, et al. Sources of aeolian magnetite at a remote site in Japan: Dominantly Asian desert dust or anthropogenic emissions? *Atmospheric Environment*. 2023, 314: 120093.
40. Li S, Zhang B, Wu D, et al. Magnetic particles unintentionally emitted from anthropogenic sources: iron and steel plants. *Environmental Science & Technology Letters*. 2021, 8(4): 295-300.
41. Data collection of Past Weather by Japan Meteorological Agency (in Japanese). Available online: <https://www.data.jma.go.jp/stats/etrn/index.php> (accessed on 2 October 2024).